# Optical Spectroscopy of Single Impurity Centers in Semiconductors

S. Francoeur,[1,*] J. F. Klem,[2] and A. Mascarenhas[1]
[1]National Renewable Energy Laboratory, Golden, Colorado 80401, USA
[2]Sandia National Laboratory, Albuquerque, New Mexico 87185, USA
(Received 26 February 2004; published 5 August 2004)

Using optical spectroscopy with diffraction limited spatial resolution, the possibility of measuring the luminescence from single impurity centers in a semiconductor is demonstrated. Selectively studying individual centers that are formed by two neighboring nitrogen atoms in GaAs makes it possible to unveil their otherwise concealed polarization anisotropy, analyze their selection rules, identify their particular configuration, map their spatial distribution, and demonstrate the presence of a diversity of local environments. Circumventing the limitation imposed by ensemble averaging and the ability to discriminate the individual electronic responses from discrete emitters provides an unprecedented perspective on the nanoscience of impurities.

DOI: 10.1103/PhysRevLett.93.067403 PACS numbers: 78.67.Hc, 71.55.Eq, 78.55.Et

The ability to probe single, isolated and spatially resolved entities permits the observation of their intrinsic, singular, and hidden properties otherwise masked by ensemble averaging. This has led to remarkable progress in the understanding of atoms [1,2] molecules [3,4], defects [5], and quantum dots [6–8]. While single impurities or defects have been observed in polymers [3] and insulators [5], little appears to be known about the characteristics of single impurities in semiconductors. We report on the fine structure luminescence from single isolated nitrogen pairs in GaAs measured using a confocal microscope. Spectrally and spatially resolving luminescent centers lifts the orientational degeneracy, reveals critical information on their symmetry and configuration, and exposes their distinctive signatures. In addition, the spatial distribution of impurities can be reconstructed. This approach provides information previously unattainable for understanding the physics of semiconductors at a scale of single impurity centers [9].

The measurement of a single molecule, dot, or impurity, by optical spectroscopy represents a formidable task requiring two fundamental requirements to be satisfied. First, the density must be such that only one luminescent entity is located within the excitation or detection volume. Next, the photon emission rate from a single recombination center must be fast enough to provide a signal exceeding noise levels. Nitrogen pairs in GaAs satisfy both requirements. Despite being isovalent with As, nitrogen forms localized bound states in GaAs [10] and so is referred to as an isoelectronic impurity. The disparity in core electronic potentials and lattice relaxation resulting from its substitution create a localized potential attractive to an electron which consequently can capture a hole to form an exciton. When two neighboring nitrogen atoms are located on the anion sublattice, referred to as a nitrogen pair, they can trap excitons with a binding energy strongly dependent on the nitrogen pair separation [11,12]. Without hydrostatic pressure, most of these pair states are resonant in the conduction band and only two nitrogen pair configurations form bound states [13]. Although the minimum nitrogen doping level routinely achievable (around $10^5\ \mu m^{-3}$) is exceedingly high even for sampling volumes obtained using near-field optical techniques, the nitrogen pair concentration for this same doping level is $3\ \mu m^{-3}$, corresponding to a sampling volume easily achievable using diffraction limited optical techniques.

The sample was grown by molecular beam epitaxy, and its structure corresponds to a 25 nm GaAs:N layer, clad by a protective 5 nm of GaAs on both sides, and sandwiched between two $Al_{0.25}Ga_{0.75}As$ barriers. From secondary ion mass spectrometry on thicker calibration samples, the nitrogen concentration was estimated to be $3 \times 10^5\ \mu m^{-3}$, corresponding to a pair surface density of $0.6\ \mu m^{-2}$. The luminescence excitation was performed at 532 nm using an intensity of 90 nW with a resolution of $0.5\ \mu m^2$. Because of the long carrier diffusion length at 5 K, the spatial resolution for the detection of the luminescence is set by the 10 $\mu$m pinhole located in an intermediate image plane, resulting in a detection resolution of $0.64\ \mu m^2$. Figure 1(a) shows spectra selected from three different locations on a $5 \times 5\ \mu m^2$ photoluminescence (PL) map. Two types of centers are observed and correspond to pairs with discrete but different separations. They are referred to as $NN_1$ and $NN_2$ and, while their configuration has not yet been established, they likely correspond to pair arrangements wherein if a nitrogen atom is located at the origin, the pair atom is located at either (1/2, 1/2, 0) or (1, 1, 0) of the anion sublattice. If this configuration is exact, these pairs should then have and a $C_{2v}$ symmetry. We use $X_1$ and $X_2$ to refer to these radiative centers and arbitrarily assign $X_2$ to the lower energy one. The three panels of Fig. 1(a) show one $X_2$ center and two distinct $X_1$ centers labeled $X_1^{(1)}$ and $X_1^{(2)}$. For both $X_1$ and $X_2$, the exchange split $A$ ($J = 1$ triplet) and $B$ ($J = 2$ quintet) states further split under the biaxial

 0031-9007/04/93(6)/067403(4)$22.50  

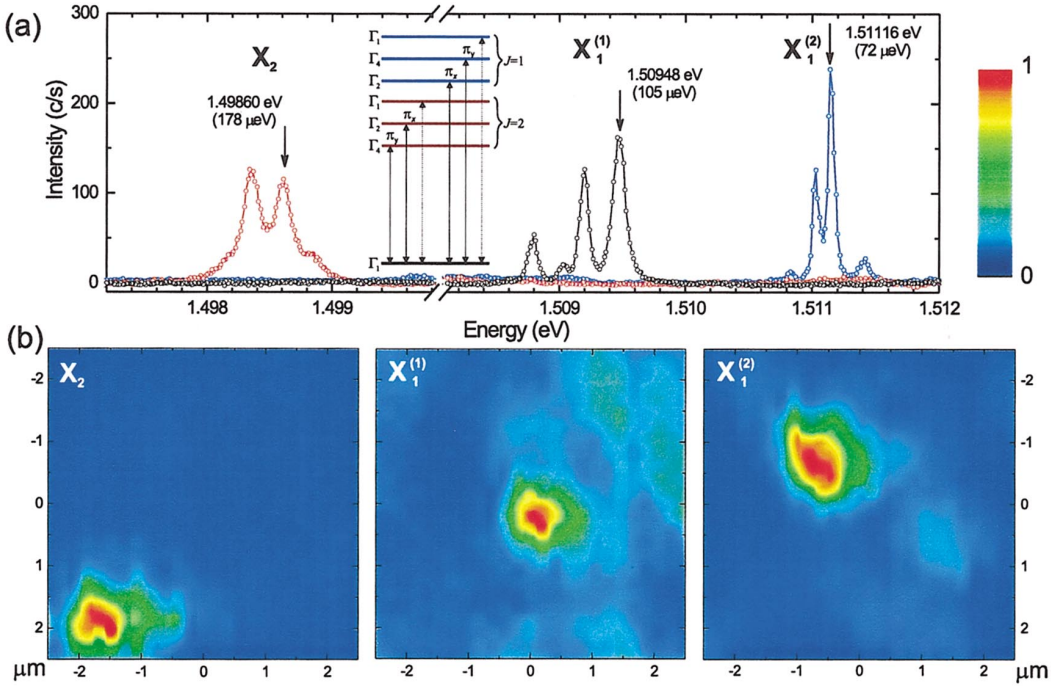


FIG. 1 (color). (a) Photoluminescence spectra obtained from three different regions of a 25 $\mu m^2$ spatial map. $X_1^{(1)}$, $X_1^{(2)}$, and $X_2$ correspond to three distinct nitrogen pairs. $X_1$ and $X_2$ are two pairs with discrete but different separation. Inset: linearly polarized optical transitions for $C_{2v}$ symmetry. The photon wave vector is along $z$, the $C_2$ axis, and the pair is oriented along $x$. (b) Photoluminescence intensity maps corresponding to pairs $X_1^{(1)}$, $X_1^{(2)}$, and $X_2$. The intensity is plotted for the luminescence peaks shown by arrows on the spectra in (a).

crystal field into eight singlets. Two transitions from the $J = 2$ to the $J = 0$ ground state are forbidden whereas the remaining six can in principle be observed. The inset of Fig. 1(a) shows the symmetry of each exciton state [14] assuming the crystal field lifts all degeneracies. The ordering of the six singlets is not accurately known. Assuming that only one nitrogen pair is located in the luminescence detection volume and that the orientation of the pair is perpendicular to the luminescent photon's wave vector, only four of the six transitions should be observed. Indeed, four luminescence peaks are clearly identified for $X_1^{(1)}$ and $X_1^{(2)}$, whereas for $X_2$ the presence of four peaks is illustrated below. The above gap excitation energy likely creates a nonequilibrium phonon population, broadening the individual lines beyond their natural linewidth.

Figure 1(b) shows one spatial intensity map for each center measured at an energy corresponding to the luminescence features indicated by the arrows on the spectra in Fig. 1(a). The scanning step size was 0.2 $\mu$m, but Fig. 1(b) shows an interpolated step size of 0.05 $\mu$m. The PL maps were obtained by integrating the intensity within a 92 $\mu$eV energy window. An identical localization of the four spectral features indicates they all originate from the same emitter. This demonstrates that the relatively high spectral and spatial resolution allows us to probe the distribution of single impurity centers in a semiconductor. The luminescence intensity saturates at excitation intensities exceeding 18 nW. While luminescence intermittency is often observed from single emitters [6,15], no intensity fluctuations are observed nor expected since the configuration of the pairs and their environments are stable under normal excitation levels and long-lived nearby carrier traps should not be present. Previous impurity-related luminescence measurements probed a large collection of emitters and the information related to their symmetry and orientation was lost through ensemble averaging. In some cases, as, for example, donor-acceptor pairs [16], partially polarized luminescence is observed due to the influence of a growth-related preferential incorporation favoring some configurations over others. In contrast, spatially resolving a single luminescent center completely lifts the orientational degeneracy, facilitating the analysis of the optical selection rules and nearly degenerate states.

For $C_{2v}$ symmetry, the dipole moment operator mediating an optical transition between any of the electronic states produces linearly polarized luminescence. Figure 2 shows the intensity of the photoluminescence as a function of energy and polarization angle for the three centers of Fig. 1. Four transitions are observed for each center, two related to the $B$ ($J = 2$) exciton at low energy and two related to the $A$ ($J = 1$) exciton at high energy [17]. We observe a striking variation of the intensity of these

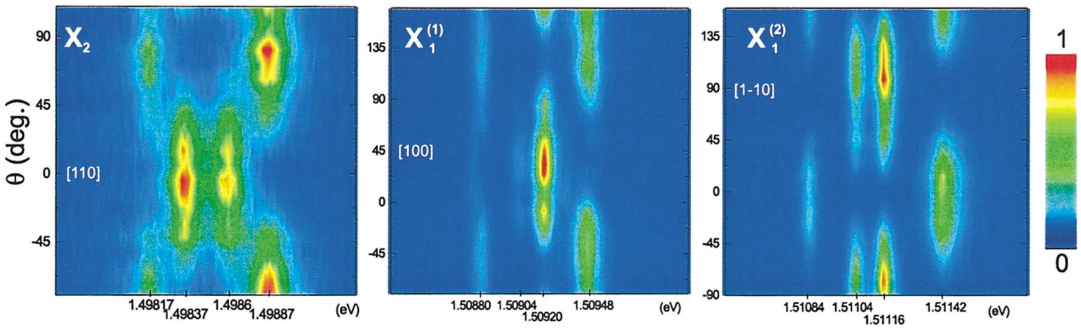


FIG. 2 (color). Photoluminescence intensity as a function of energy and polarization angle. 0°, 45°, and 90° corresponds to [110], [100], and [1-10], respectively. The four transitions allowed from $C_{2v}$ symmetry are resolved. As can be clearly seen from all three panels, the polarization anisotropy ratio reaches unity. This demonstrates that the orientational degeneracy is lifted, as expected for a single emitter.

transitions with polarization angle for all centers. As expected, the polarization intensity varies from zero (forbidden transitions) to a maximum value (allowed transitions). The relative orientation of the pairs can be determined from their polarization characteristics. Since the emitted light is polarized along ($\pi_x$) or perpendicular to the pair ($\pi_y$), we find that $X_1^{(2)}$ and $X_2$ are located in the (001) plane but oriented perpendicularly to each other, whereas $X_1^{(1)}$ is located in the (100) plane. The crystallographic orientation of the pairs and their polarization selection rules indeed favors a $C_{2v}$ symmetry for both $X_1$ and $X_2$. This demonstrates that the polarization anisotropy, concealed in macroscopic measurements, provides critical information on the impurity configuration.

It is natural to expect that the local environment of a nitrogen impurity pair will affect the energy of its luminescence. The presence of charged impurities, lattice distortions, strains, and other local fields affects the properties of the host semiconductor on a very short length scale. The presence of these nonresolved local perturbations on the host electronic states is usually analyzed through linewidth broadening even at the highest spatial resolutions achievable by optical spectroscopy. The ability to spatially resolve individual impurity centers could thus serve as a nanoscopic probe for the analysis of these perturbations with unprecedented spatial resolution as demonstrated below. The electron, tightly bound to nitrogen [18], has a large mass and the exciton radius is less than 4 nm [19], implying that the characteristics of the nitrogen bound exciton should be minimally affected by perturbations outside this radius.

As can be seen from Fig. 1(a), the central position of the luminescence is remarkably different for $X_1^{(1)}$ and $X_1^{(2)}$. Since the spacing between the nitrogen atoms can assume only discrete values, we attribute this difference in energy to the variation in local environments. From a macro-PL measurement (area of approximately 1200 $\mu m^2$), we find that $X_1$ broadens to a single unresolved line at 1.507 94 eV (not shown) [20]. This energy represents an ensemble average from approximately 1000 pairs. We then calculate the energy separation between the average value of the four excitonic lines and the macro-PL ensemble average energy. Figure 3 shows a color-coded energy variation map (same sample region shown in Fig. 1). Each circle represents the location of a $X_1$ center and its color indicates the magnitude of the energy shift. In this particular region of the sample, the energy shift is mostly towards positive values with an average of +1.513 meV. This indicates the presence of a relatively long scale perturbation (>5 $\mu$m) shifting most of these peaks to higher energy. It also appears that there is little spatial correlation between the energy of each data point, indicating that significantly shorter scale perturbations are also present (<1 $\mu$m). Their effects vary rapidly on the scale of the probes' surface density. These two types of perturbations are likely to originate from strain fields, uniaxial or

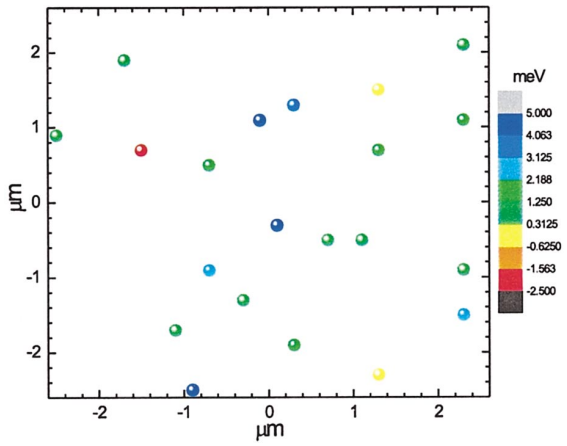


FIG. 3 (color). Spatial location map of $X_1$ centers from the same area shown in Fig. 1(b). The energy shift of $X_1$ with respect to the average energy obtained through a macro-PL measurement (large ensemble) is shown (see color scale). Large scale (>5 $\mu$m) and short scale (<1 $\mu$m) perturbations can be identified. Nitrogen pairs provide a very sensitive measurement of the host perturbation with a nanometer scale resolution.

biaxial, impurities, or any other defect generating lattice distortions. This rapid variation and its large amplitude can probably be in part associated with the relatively low growth temperature for this sample which often results in a lower crystalline quality and explains the observation of just a single broadened unresolved line in the macro-PL measurement. Interestingly, we find the exchange interaction and crystal-field splitting are also strongly affected by their local environment. By associating the experimental results with theoretical models, the luminescence energy, the exchange interaction, and crystal-field splitting could be used to investigate the presence of strain and electrical fields with extremely high resolution.

The surface density of $X_1$ is estimated to be 0.84 $\mu m^{-2}$ from Fig. 3. An analysis of the spatial surface distribution of the nitrogen centers gives a nearest neighbor index of 1.23 [21]. While a random spatial distribution is often assumed, the deviation of this value from unity indicates an intermediate tendency to scatter which is perhaps controlled by the dynamics at the growth surface. This tendency is highly favorable from a practical standpoint because a uniform distribution of dopants is preferred for optimal carrier transport in devices and, at higher concentrations where alloy formation begins, clustering would induce local energy fluctuations of electronic bands resulting in broadened densities of states. Although limited to two dimensions, it appears this approach can provide valuable insight into the local environment of impurities, the statistics of dopant distribution, and help shed light on the puzzling electronic structure evolution in the embryonic phase of the ultradilute GaAsN alloy.

In summary, we have probed the fine-structure luminescence of single nitrogen pairs in GaAs. Spectrally and spatially resolving the luminescent centers lifts the orientational degeneracy, revealing critical information on their symmetry, configuration, and distribution. The signature of an impurity center is sensitive to its environment and could be used as a marker revealing the presence of nearby impurities, defects, strain, or electrical fields, with a sensitivity and resolution unattainable using other techniques.

We acknowledge support from the Office of Science of the U.S. Department of Energy under Contract No. DE-AC36-83CH10093 and from the National Center for Photovoltaics. Sandia is a multiprogram laboratory operated by Sandia Corporation, a Lockheed Martin Company, for the U.S. Department of Energy's National Nuclear Security Administration under Contract No. DE-AC04-94AL85000.

*Electronic address: sebastien_francoeur@nrel.gov

[1] H. Kimble, M. Dagenais, and L. Mandel, Phys. Rev. Lett. **39**, 691 (1977).
[2] J. Bergquist, R. G. Hulet, W. Itano, and D. Wineland, Phys. Rev. Lett. **57**, 1699 (1986).
[3] W. Moerner and L. Kador, Phys. Rev. Lett. **62**, 2535 (1989).
[4] S. Weiss, Science **283**, 1676 (1999).
[5] A. Gruber, A. Drabenstedt, C. Tietz, L. Fleury, J. Wrachtrup, and C. von Borczyskowski, Science **276**, 2012 (1997).
[6] M. Nirmal, B. Dabbousi, M. Bawendi, J. Macklin, J. Trautman, T. Harris, and L. Brus, Nature (London) **383**, 802 (1996).
[7] L. Landin, M. Miller, M.-E. Pistol, C. Pryor, and L. Samuelson, Science **280**, 262 (1998).
[8] M. Bayer, O. Stern, P. Hawrylak, S. Fafard, and A. Forchel, Nature (London) **405**, 923 (2000).
[9] M. Castell, D. Muller, and P. Voyles, Nature Mater. **2**, 129 (2003).
[10] D. Wolford, K. Fry, and J. Thompson, *The Nitrogen Isoelectronic Trap in GaAs* (Spinger- Verlag, New York, 1985), p. 627.
[11] D. Thomas and J. Hopfield, Phys. Rev. **150**, 680 (1966).
[12] X. Liu, M.-E. Pistol, and L. Samuelson, Appl. Phys. Lett. **56**, 1451 (1990).
[13] R. Schwabe, W. Seifert, F. Bugge, and R. Bindemann, Solid State Commun. **5**, 167 (1985).
[14] G. Koster, J. Dimmock, R. Wheeler, and H. Statz, *Properties of The Thirty-Two Point Groups* (MIT Press, Cambridge, 1963).
[15] W. Moerner and M. Orrit, Science **283**, 1670 (1999).
[16] M. Skolnick, C. Tu, and T. Harris, Phys. Rev. B **33**, 8468 (1986).
[17] Just as for the case of nitrogen in GaP, the crystal-field splitting is expected to be smaller than the electron-hole exchange interaction [11].
[18] P. Kent and A. Zunger, Phys. Rev. B **64**, 115208 (2001).
[19] A. Baldareshi and N. Lipari, Phys. Rev. B **8**, 2697 (1973).
[20] S. Fafard, R. Leon, D. Leonard, J. Merz, and P. Petroff, Nature (London) **383**, 802 (1996).
[21] An index of 1 represents a random distribution, whereas 0 and 2.15 correspond to a perfectly clustered and uniform distribution. The index was corrected for the size of the perimeter (uncorrected index: 1.35).